Searches for heavy neutral lepton production at the NA62 experiment

Christopher John Parkinson[a,∗]

[a]*Centre for Cosmology, Particle Physics and Phenomenology, Université catholique de Louvain, Louvain-la-Neuve, Belgium*

E-mail: chris.parkinson@cern.ch

Searches for heavy neutral lepton production in $K^+ \to e^+ N$ and $K^+ \to \mu^+ N$ decays using the data set collected by the NA62 experiment at CERN in 2016-18 are presented. Upper limits on the elements of the extended neutrino mixing matrix and are established at the levels of 10^{-9} and 10^{-8}, respectively, improving on the earlier searches for heavy neutral lepton production and decays in the kinematically accessible mass range. Searches for the $K^+ \to \mu^+ \nu \nu \bar{\nu}$ and $K^+ \to \mu^+ \nu X$ decays, where X is a new light invisible particle, are also reported.

∗Speaker, for the NA62 Collaboration: A. Akmete, R. Aliberti, F. Ambrosino, R. Ammendola, B. Angelucci, A. Antonelli, G. Anzivino, R. Arcidiacono, T. Bache, A. Baeva, D. Baigarashev, L. Bandiera, M. Barbanera, J. Bernhard, A. Biagioni, L. Bician, C. Biino, A. Bizzeti, T. Blazek, B. Bloch-Devaux, P. Boboc, V. Bonaiuto, M. Boretto, M. Bragadireanu, A. Briano Olvera, D. Britton, F. Brizioli, M.B. Brunetti, D. Bryman, F. Bucci, T. Capussela, J. Carmignani, A. Ceccucci, P. Cenci, V. Cerny, C. Cerri, B. Checcucci, A. Conovaloff, P. Cooper, E. Cortina Gil, M. Corvino, F. Costantini, A. Cotta Ramusino, D. Coward, G. D'Agostini, J. Dainton, P. Dalpiaz, H. Danielsson, M. D'Errico, N. De Simone, D. Di Filippo, L. Di Lella, N. Doble, B. Dobrich, F. Duval, V. Duk, D. Emelyanov, J. Engelfried, T. Enik, N. Estrada-Tristan, V. Falaleev, R. Fantechi, V. Fascianelli, L. Federici, S. Fedotov, A. Filippi, R. Fiorenza, M. Fiorini, J. Fry, J. Fu, A. Fucci, L. Fulton, E. Gamberini, L. Gatignon, G. Georgiev, S. Ghinescu, A. Gianoli, M. Giorgi, S. Giudici, F. Gonnella, K. Gorshanov, E. Goudzovski, C. Graham, R. Guida, E. Gushchin, F. Hahn, H. Heath, J. Henshaw, Z. Hives, E.B. Holzer, T. Husek, O. Hutanu, D. Hutchcroft, L. Iacobuzio, E. Iacopini, E. Imbergamo, B. Jenninger, J. Jerhot, R.W. Jones, K. Kampf, V. Kekelidze, D. Kerebay, S. Kholodenko, G. Khoriauli, A. Khotyantsev, A. Kleimenova, A. Korotkova, M. Koval, V. Kozhuharov, Z. Kucerova, Y. Kudenko, J. Kunze, V. Kurochka, V. Kurshetsov, G. Lanfranchi, G. Lamanna, E. Lari, G. Latino, P. Laycock, C. Lazzeroni, M. Lenti, G. Lehmann Miotto, E. Leonardi, P. Lichard, L. Litov, P. Lo Chiatto, R. Lollini, D. Lomidze, A. Lonardo, P. Lubrano, M. Lupi, N. Lurkin, D. Madigozhin, I. Mannelli, A. Mapelli, F. Marchetto, R. Marchevski, S. Martellotti, P. Massarotti, K. Massri, E. Maurice, A. Mazzolari, M. Medvedeva, A. Mefodev, E. Menichetti, E. Migliore, E. Minucci, M. Mirra, M. Misheva, N. Molokanova, M. Moulson, S. Movchan, M. Napolitano, I. Neri, F. Newson, A. Norton, M. Noy, T. Numao, V. Obraztsov, A. Okhotnikov, A. Ostankov, S. Padolski, R. Page, V. Palladino, I. Panichi, A. Parenti, C. Parkinson, E. Pedreschi, M. Pepe, M. Perrin-Terrin, L. Peruzzo, P. Petrov, Y. Petrov, F. Petrucci, R. Piandani, M. Piccini, J. Pinzino, I. Polenkevich, L. Pontisso, Yu. Potrebenikov, D. Protopopescu, M. Raggi, M. Reyes Santos, M. Romagnoni, A. Romano, P. Rubin, G. Ruggiero, V. Ryjov, A. Sadovsky, A. Salamon, C. Santoni, G. Saracino, F. Sargeni, S. Schuchmann, V. Semenov, A. Sergi, A. Shaikhiev, S. Shkarovskiy, M. Soldani, D. Soldi, M. Sozzi, T. Spadaro, F. Spinella, A. Sturgess, V. Sugonyaev, J. Swallow, A. Sytov, G. Tinti, A. Tomczak, S. Trilov, P. Valente, B. Velghe, S. Venditti, P. Vicini, R. Volpe, M. Vormstein, H. Wahl, R. Wanke, V. Wong, B. Wrona, O. Yushchenko, M. Zamkovsky, A. Zinchenko.

1. Introduction

All Standard Model (SM) fermions except neutrinos are known to exhibit right-handed chirality. The existence of right-handed neutrinos, or heavy neutral leptons (HNLs), is hypothesised in many SM extensions in order to generate non-zero masses of the SM neutrinos via the seesaw mechanism. For example, the Neutrino Minimal Standard Model simultaneously accounts for dark matter, baryogenesis, and neutrino masses and oscillations by postulating two HNLs in the MeV − GeV mass range and a third HNL, a dark matter candidate, at the keV mass scale [1]. Mixing between HNLs and active neutrinos gives rise to HNL production in decays of SM particles and decays of HNLs into SM particles. The decay $K^+ \rightarrow \ell^+ N$ ($\ell = e, \mu$) has the branching fraction [2]

$$\mathcal{B}(K^+ \rightarrow \ell^+ N) = \mathcal{B}(K^+ \rightarrow \ell^+ \nu) \cdot \rho_\ell(m_N) \cdot |U_{\ell 4}|^2, \tag{1}$$

where N denotes an HNL, $\mathcal{B}(K^+ \rightarrow \ell^+ \nu)$ is the measured branching fraction of the SM leptonic decay, $|U_{\ell 4}|^2$ is the mixing parameter, m_N is the HNL mass, and $\rho_\ell(m_N)$ is a kinematic factor defined as

$$\rho_\ell(m_N) = \frac{(x+y) - (x-y)^2}{x(1-x)^2} \cdot \lambda^{1/2}(1, x, y), \tag{2}$$

with $x = (m_\ell/m_K)^2$, $y = (m_N/m_K)^2$ and $\lambda(a, b, c) = a^2 + b^2 + c^2 - 2(ab + bc + ac)$. The value of $\rho_\ell(m_N)$ is 1 when $m_N = 0$, rises to a maximum of about 4 when $m_N \approx 250\,\text{MeV}/c^2$, then quickly falls to 0 as the kinematic limit $m_N = m_K - m_\ell$ is approached. With conservative assumptions on the value of the mixing parameters, the HNL lifetime is expected to be more than 1μs, making them effectively stable for production searches.

A new light gauge boson has been proposed as an explanation of the muon $g - 2$ anomaly [3]. A particular scenario, which also accommodates dark matter (DM) freeze-out, involves a scalar or vector boson X that couples preferentially to the muon. If $m_X < m_K - m_\mu$, the new particle is expected to be produced in $K^+ \rightarrow \ell^+ \nu X$ decays with an estimated branching fraction of $O(10^{-8})$. The X boson will subsequently decay with a sizeable invisible branching fraction [4]. In the light DM freeze-out model the decay $X \rightarrow \chi\chi$ is expected, where χ is a dark matter candidate.

The strongest limit on the $K^+ \rightarrow \mu^+ \nu\nu\bar{\nu}$ branching fraction was set at $\mathcal{B}(K^+ \rightarrow \mu^+ \nu\nu\bar{\nu}) < 2.4 \times 10^{-6}$ at 90% CL by the BNL-E949 experiment [5]. This limit is several orders of magnitude larger than the $O(10^{-16})$ branching fraction expected in the SM, motivating further examination [6].

The NA62 experiment is located in the CERN North Area and uses a decay-in-flight technique to study K^+ decays [7]. An unseparated beam of positively charged kaons (6%), pions (70%) and protons (23%) is obtained by impinging a proton beam extracted from the CERN SPS onto a fixed beryllium target. The central beam momentum is 75 GeV/c, with a momentum spread of 1% (rms). The beam is directed through a kaon tagger (KTAG) and beam spectrometer (GTK) to measure the properties of the incoming kaons, followed by a large vacuum tank in which a $\sim$ 75m fiducial volume (FV) is defined. The products of kaon decays in the FV pass through a STRAW spectrometer that measures the momenta of the charged decay products, follwed by a Ring Imaging Cherenkov detector (RICH), two charged-particle hodoscopes (CHOD), a liquid krypton calorimeter (LKr), and a muon detector system. In addition, the FV is surrounded by a hermetic photon veto system. NA62 has collected more than 10^{12} K^+ decays during 3 years of operations in 2016-2018.

This document reports the study of the $K^+ \to \ell^+ N$, $K^+ \to \ell^+ \nu X$, and $K^+ \to \mu^+ \nu \nu \bar{\nu}$ decays using the data set collected at NA62 [8, 9]. Each of the decays is characterised by a single positively-charged lepton (e, μ) and missing energy. The N particle is interpreted as a HNL, and results are presented in terms of upper limits on the mixing parameter $|U_{\ell 4}|^2$ under the assumption that the HNL lifetime exceeds 50 ns. The X particle is interpreted as a new boson, either vector or scalar, and results are presented in terms of upper limits on the $K^+ \to \ell^+ \nu X$ branching fraction.

2. Event selection and measurement strategy

Events that contain the signature of a K^+ decay to a single-track final state were isolated in the NA62 data sample by selecting those that contained the track of a positively charged particle reconstructed in the STRAW spectrometer. The excellent particle identification capabilities of the NA62 detector were used to select those tracks produced by charged leptons. Positive muons were required to have: the track momentum measured by the STRAW spectrometer (p) to be within $5 - 70$ GeV/c; the ratio of the energy deposited in the LKr (E) to the particle momentum p to be $E/p < 0.2$; and a hit in the muon detector that is consistent with the reconstructed track in both time and position. Positrons were required to have: the track momentum p in the range $5 - 30$ GeV/c; the E/p in the range $0.92 - 1.08$; and no hit in the muon detector that is consistent with the track in time and position. For those charged leptons below 30 GeV/c, a particle identification algorithm based on information from the RICH detector was also applied to distinguish muons from positrons. Backgrounds from beam pions were suppressed by requiring a K^+ candidate reconstructed in the KTAG that is consistent in time with the reconstructed lepton. The K^+ track was reconstructed in the GTK, and events were rejected if the reconstructed K^+ track was not consistent in time and position with the reconstructed lepton. The decay vertex was defined as the point of closest approach between the reconstructed K^+ and lepton tracks. Background from $K^+ \to \mu^+ \nu$ decays (with subsequent decay of the muon, in the positron case) were suppressed by imposing a condition on the position of the decay vertex as a function of the angle between the K^+ momentum in the lab frame and the lepton momentum in the K^+ rest frame. Finally, backgrounds from multi-body K^+ decays were suppressed by veto conditions imposed on other tracks reconstructed by the STRAW spectrometer, additional energy deposits in the LKr, energy deposits in the photon veto system, and additional signals in the CHOD.

As the incoming K^+ and outgoing charged lepton are both reconstructed in the NA62 experiment, the squared missing mass m_{miss}^2 can be precisely computed as $m_{\text{miss}}^2 = P_K^2 - P_\ell^2$, where $P_{K,\ell}$ are the squared four-momenta of the K^+ and charged lepton, respectively. The m_{miss}^2 distribution is plotted in Fig. 2 for the positron case (left) and the muon case (right). The SM $K^+ \to \ell^+ \nu$ decays are seen as striking peaks at $m_{\text{miss}}^2 = 0$. The selection yielded 3.495×10^6 $K^+ \to e^+ \nu$ candidates and 2.19×10^9 $K^+ \to \mu^+ \nu$ candidates. The m_{miss}^2 distribution of the positron candidates exhibits a sharp increase at a threshold of around $m_{\text{miss}}^2 = 0.13$ GeV^2/c^4 due to background from beam pion decays. The threshold at which this background appears depends simply on the maximum positron momentum, hence, an 'auxiliary' selection was defined that imposed a maximum momentum requirement of < 20 GeV/c on the positron candidates. While the auxiliary criteria have lower selection efficiency, it allows the m_{miss}^2 region just above 0.13 GeV^2/c^4 to be probed without the overwhelming pion decay background. Meanwhile, the m_{miss}^2 distribution of the muon candidates exhibits a deficit of simulated events in the non-gaussian tails on the negative-side of the $K^+ \to \mu^+ \nu$

m_{miss}^2 distribution, resulting from the limited precision in the simulation of beam-particle pileup and inefficiency in the GTK. Under the assumption that the non-gaussian tails are symmetric, a 'tail' component was added to the estimated background on the positive side, shown in orange in Fig. 2 (right). This tail component was assigned a 100% systematic uncertainty.
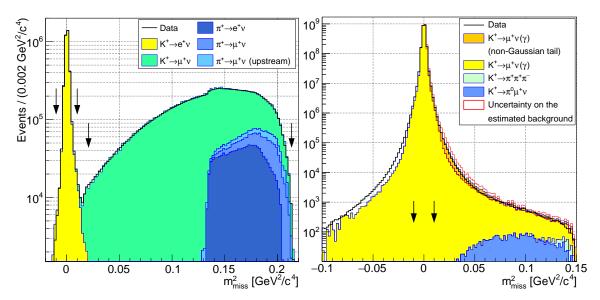

Figure 1: Reconstructed m_{miss}^2 distribution of $K^+ \to e^+\nu$ (left) and $K^+ \to \mu^+\nu$ (right) candidates in data (black line) and simulated events (coloured areas), from [8] and [9], respectively.

Any $K^+ \to \ell^+ N$ decays would appear as a peak on the positive side of the m_{miss}^2 distribution. The HNL search is performed in just over 260 regions of m_{miss}^2, with the width of each region defined as $1.5\sigma_{\text{m}}$, where σ_{m} is the m_{miss}^2 mass resolution at the given value of m_N. In the muon case the search regions are distributed between $200 - 384 \, \text{MeV}/c^2$ with centres separated by $1(0.5) \, \text{MeV}/c^2$ below (above) $300 \, \text{MeV}/c^2$, while for the positron case, the search regions are distributed between $144 - 462 \, \text{MeV}/c^2$ with centres separated by σ_{m}. The background in each search region is evaluated by 2nd order polynomial fits to the data in the region between $1.5\sigma_{\text{m}} < |m_{\text{miss}}^2 - m_N| < 11.25\sigma_{\text{m}}$. In the positron case, the auxiliary selection was used when close to the threshold of the pion decay background to ensure good fits to the background were obtained. The number of events observed, the expected background, and the uncertainty on the expected background, are used to compute the upper limit on the number of $K^+ \to \ell^+ N$ decays in each search region using the CLs method. The limits obtained are shown in Fig. 2 for the positron case (left) and the muon case (right). The results are also interpreted as limits on the mixing parameters $|U_{e4}|^2$ and $|U_{\mu4}|^2$, which are compared to previous limits in Fig. 3.

The m_{miss}^2 distribution of the $K^+ \to \ell^+ \nu X$ and $K^+ \to \mu^+ \nu \nu \bar{\nu}$ decays are shown in Fig. 4 (left). Both decays exhibit a broad spectrum of large positive m_{miss}^2. In the $K^+ \to \ell^+ \nu X$ case, the mass of the X boson leads to a lower threshold at $m_{\text{miss}}^2 = m_X$. The search for the X boson is performed with 37 m_X hypotheses equally spaced between $10 - 370 \, \text{MeV}/c^2$. Both scalar and vector bosons are considered. For the $K^+ \to \ell^+ \nu X$ decay search with m_X in the range $320 - 270 \, \text{MeV}/c^2$, the lower edge of the signal region (m_0^2) is defined as $m_0^2 = m_X^2$. For the $K^+ \to \ell^+ \nu X$ decay search with m_X in the range $10 - 310 \, \text{MeV}/c^2$, as well as the search for the $K^+ \to \mu^+ \nu \nu \bar{\nu}$ decay, the signal
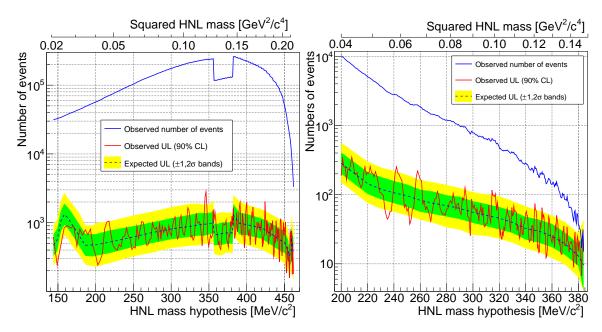
Figure 2: The observed number of events (blue line), the observed upper limit at 90% CL (red line), and the expected limit (black dashed line) with its associated 1σ and 2σ bands (green, yellow coloured areas) for the $K^+ \to e^+ N$ (left) and $K^+ \to \mu^+ N$ (right) searches, from [8] and [9], respectively.
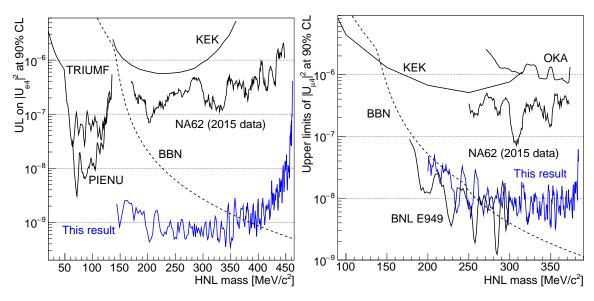

Figure 3: Observed upper limits at 90% CL on the mixing parameters $|U_{e4}|^2$ (left) and $|U_{\mu4}|^2$ (right) compared to the existing world knowledge, from [8] and [9], respectively.

region is defined from $m_0^2 = 0.1\,\text{GeV}/c^2$. Upper limits on $\mathcal{B}(K^+ \to \ell^+ \nu X)$ are set using the CLs method, with the expected background and its uncertainty evaluated using simulated events. These limits are shown in Fig. 4 (right). The limits obtained in the scalar model are stronger due to the larger mean m_{miss}^2 value. In the search for the $K^+ \to \mu^+ \nu \nu \bar{\nu}$ decay, 6894 events are observed in the signal region, with an expected background of 7549 ± 928 events. This leads to an observed limit of $\mathcal{B}(K^+ \to \mu^+ \nu \nu \bar{\nu}) < 1.0 \times 10^{-6}$ at 90% CL, improving on the previous most stringent limit by a factor of 2.4 in a complementary range of m_{miss}^2.
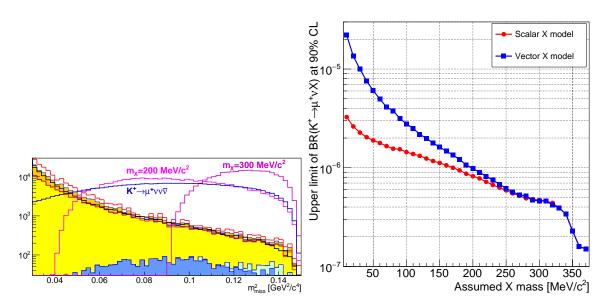
Figure 4: Left panel: expected m^2_{miss} distribution of $K^+ \to \mu^+\nu\nu\bar{\nu}$ decays (blue line) and $K^+ \to \ell^+\nu X$ decays with two m_X hypotheses (pink lines), overlaid on the reconstructed m^2_{miss} distribution of $K^+ \to \mu^+\nu$ candidates in data (black line) and simulated events (coloured areas), from [9]. Right panel: observed upper limit on $\mathcal{B}(K^+ \to \ell^+\nu X)$ as a function of m_X, assuming a scalar (red points) or vector (blue points) X boson, from [9].

3. Summary

Improved limits at the level of 10^{-9} were set on the HNL mixing parameter $|U_{e4}|^2$ in the mass range $144 - 462$ MeV/c^2. These are the world's best limits in this mass range, which excludes the region favoured by Big Bang Nucleosynthesis (BBN) up to ~ 340 MeV/c^2. Improved limits were also set on the HNL mixing parameter $|U_{\mu 4}|^2$ at the level of 10^{-8} in the mass range $200 - 384$ MeV/c^2, which constitute the world's best limits on this parameter above 300 MeV/c^2. The first ever limits were set on the branching fraction of the $K^+ \to \ell^+\nu X$ decay, with X either a scalar or vector boson with mass in the range $10 - 370$ MeV/c^2 that decays to invisible particles. Finally, the limit of $\mathcal{B}(K^+ \to \mu^+\nu\nu\bar{\nu}) < 1.0 \times 10^{-6}$ was set at 90% CL, improving on earlier limits and probing a complementary region of m^2_{miss}.

References

[1] T. Asaka and M. Shaposhnikov, Phys. Lett. B 620 (2005) 17.

[2] R. Shrock, Phys. Lett. B 96 (1980) 159; Phys. Rev. D 24 (1981) 1232.

[3] S.N. Gninenko and N.V. Krasnikov, Phys. Lett. B 513 (2001) 119.

[4] G. Krnjaic et al., Phys. Rev. Lett. 124 (2020) 041802.

[5] A.V. Artamomov et al., Phys. Rev. D 94 (2016) 032012.

[6] D. Gorbunov and A. Mitrofanov, J. High Energy Phys. 1610 (2016) 039.

[7] E. Cortina Gil et al., J. Instrum. 12 (2017) P05025.

[8] E. Cortina Gil et al., Phys. Lett. B 807 (2020) 135599.

[9] E. Cortina Gil et al., Phys. Lett. B 816 (2021) 136259.